Investigational New Drugs **24:** 27–36, 2006.

DOI: 10.1007/s10637-005-4540-2

Effects of the tumor vasculature targeting agent NGR-TNF on the tumor microenvironment in murine lymphomas

H.W.M. van Laarhoven[1,*], G. Gambarota[2,*], A. Heerschap[2], J. Lok[3], I. Verhagen[3], A. Corti[4], S. Toma[5], C. Gallo Stampino[5], A. van der Kogel[3] and C.J.A. Punt[1]

[1]*Department of Medical Oncology, University Medical Centre Nijmegen, Nijmegen, The Netherlands;* [2]*Department of Radiology, University Medical Centre Nijmegen, Nijmegen, The Netherlands;* [3]*Department of Radiation Oncology, University Medical Centre Nijmegen, Nijmegen, The Netherlands;* [4]*Department of Biological and Technological Research, San Raffaele H Scientific Institute, Milano, Italy;* [5]*Mol Med, S.p.A., Milano, Italy*

Published online: 23 December 2005

Key words: tumor necrosis factor TNF, NGR-TNF, hypoxia, tumor microenvironment

Summary

TNF-α may improve drug delivery to tumors by alteration of vascular permeability. However, toxicity precludes its systemic administration in patients. NGR-TNF comprises TNF coupled to the peptide CNGRC, which is a ligand for CD13. CD13 is expressed on tumor vasculature. Therefore, to assess the efficacy of NGR-TNF its biological effect on tumor vasculature should be measured rather than its effect on tumor growth. The aim of this study was to assess the effects of a low dose of NGR-TNF (5 ng/kg) on vascular permeability, tumor hypoxia, perfusion and proliferation in lymphoma bearing mice. MRI measurements with blood pool contrast agent showed an increased leakage of the contrast agent from the vasculature in NGR-TNF treated tumors compared with controls ($p < 0.05$), suggesting NGR-TNF-induced vascular permeability. Immunohistochemical analysis two hours after NGR-TNF treatment showed a decrease in tumor hypoxia ($p < 0.1$) and an increase in labeling index of the S-phase marker bromodeoxyuridine ($p < 0.1$), possibly due to an increase in tumor blood flow after NGR-TNF treatment. Although a decrease in tumor hypoxia and an increase in labeling index could have lead to increased tumor growth, in this experiment after one day a decrease in tumor volume was measured. Possibly, the effects on tumor hypoxia and proliferation two hours after treatment are transient and overruled by other, more longlasting effects. For example, the observed increase in vascular permeability may lead to haemoconcentration and increased interstitial pressure, ultimately resulting in an reduction of tumor blood flow and thus a decrease in tumor growth. A beneficial effect of NGR-TNF in combination with other therapeutical agents may therefore critically depend on the sequence and timing of the regimens. Currently, NGR-TNF is being tested in clinical studies.

Introduction

The efficacy of chemotherapy depends, among other factors, on penetration of the drug into the tumor. It has been suggested that synergy between the inflammatory cytokine TNF-α and chemotherapy is based on improved drug delivery to tumors by alteration of endothelial barrier function, reduction of tumor interstitial pressure and tumor vessel damage [1–3]. A clinical proof of this concept was demonstrated in studies of isolated limb perfusion in patients with melanoma and sarcoma [4, 5]. Unfortunately, systemic treatment of TNF-α is accompanied by systemic toxicity, already at doses which are far below the therapeutic efficacy. This precludes its use in cancer patients. Targeted delivery of TNF-α to the tumor could be a way to avoid the toxicity of systemic TNF-α administration. By coupling TNF-α to CNGRC, a peptide (CD13 ligand) that targets tumor neovasculature, delivery of picogram doses of TNF-α to the tumor can be achieved [6, 7]. In murine tumor models treatment with TNF-α coupled to CNGRC (NGR-TNF) low doses of NGR-TNF showed greater inhibition of tumor growth compared to TNF, and enhanced chemotherapeutic efficacy of doxorubicin and melphalan without increasing systemic toxicity [7].

Although NGR-TNF as a single agent can decrease tumor growth [7], the drug is of clinical interest mainly because of its capacity to improve response to chemotherapy by altering tumor vasculature and tumor microenvironment.

*HvL and GG contributed equally to this work.

Therefore, for the assessment of NGR-TNF efficacy, the biological effect of NGR-TNF on tumor vasculature should be evaluated. This is especially relevant since for this class of agents the optimal biological dose may differ from the maximal tolerated dose.

The aim of this study was to assess the biological response to a low dose of NGR-TNF in lymphoma bearing mice, using dedicated magnetic resonance imaging (MRI) and immunohistochemical methods. To investigate the effect of NGR-TNF on the tumor microenvironment $T1$ and $T2$ relaxation times were measured, as they may serve as early parameters of response [8, 9]. The effect of NGR-TNF on the tumor vasculature was assessed using an ultra small iron oxide particle (USPIO) blood-pool contrast agent. The enhancement in the relaxation rates ($1/T2$ and $1/T1$) shortly after injection of USPIO, as measured by MRI, provides an index proportional to the tumor blood volume [10–15]. Furthermore, since USPIO slowly extravasates from the tumor vasculature into the interstitial space [11], the changes in $1/T2$ and $1/T1$ over time provide a measure of vessel leakage. In this way the effect of NGR-TNF on vascular permeability and NGR-TNF-induced vessel damage can be monitored. To further investigate the effect of NGR-TNF on tumor hypoxia, vasculature, perfusion and proliferation, which are parameters of the tumor microenvironment, immunohistochemical methods were used.

Materials and methods

Tumors

Mouse RMA lymphoma cells of C57/Bl6 origin were cultured as described previously [16]. 70.000 RMA lymphoma cells were injected subcutaneously in the flank of female C57BL/6 mice. Animals were kept according to institutional guidelines for animal care. When tumors had reached a diameter of at least 5 mm, experiments were started. All experiments were approved by the institutional ethical committee for animal use.

Treatment

Murine NGR-TNF (San Raffaele H Scientific Institute) was injected intraperitoneally in a dose of 100 pg/mouse in a group of 6 mice. Six mice were injected with normal saline to serve as a control. Dose-response curves where obtained by measuring tumor growth daily using callipers.

MR measurements

Since the effect of NGR-TNF on tumor growth has been observed already within one day after treatment [7], both MR and immunohistochemical measurements were performed on the same day as NGR-TNF was administered, in order to assess its biological effects.

Before the MR measurements a catheter was inserted in the tail vein of each mouse for the administration of contrast agent. After mice were anesthetized with isoflurane (1.5–2%), the tumor was positioned in the centre of a 10-mm-diameter surface RF coil which was used as a transmitter/receiver. During the measurements the body temperature was monitored with a rectal fluoroptic probe (Luxtron 712, Luxtron Corporation, California, USA). A warm water pad was used to maintain the body temperature constant. MR experiments were performed on a 7T/200 mm horizontal-bore MR spectrometer interfaced to a SMIS console.

For anatomical localization of the tumor the image acquisition protocol started with three gradient echo scout images. Then high resolution multislice gradient echo images were acquired to identify two slices of interest through the centre of the tumor. $T1$ and $T2$ relaxation times were measured before and during one hour after administration of USPIO (Figure 1, top). In particular, $T1$ relaxation times were measured at five time points — two time points before USPIO and three time points after USPIO —, while $T2$ relaxation times were measured at two time points before USPIO and two time points after USPIO.

Inversion recovery snapshot fast low angle shot (IR-FLASH) was performed to measure water $T1$ relaxation time (image matrix size 64 × 64, field of view (FOV) 3 cm × 3 cm, slice thickness (SLT) 1.6 mm, repetition time (TR) 5 ms, echo time (TE) 2.7 ms, inversion times (TI) 52 + n*320 ms, where $n = 0, 1, \ldots 15$). $T2$ relaxation times were measured with a spin echo imaging sequence (image matrix size 128 × 128, FOV 3 cm × 3 cm, SLT 1 mm, 1 signal average per phase-encoding step and TR of 1000 ms). Six images with different TE (11, 15, 20, 25, 30, 40 ms) were acquired.

The USPIO blood-pool contrast agent Sinerem® (Guerbet, France 150 μmol Fe/Kg) was injected intravenously (iv) 2 hours after treatment (Figure 1, top). This 2 hour period was chosen because a maximum effect of NGR-TNF combined with doxorubicin has been observed when doxorubicin was administered 2 hours after NGR-TNF, suggesting that a maximum effect of NGR-TNF on the vasculature was reached at that time point. (A. Corti, San Raffaele H Scientific Institute, Milano, Italy, personal communication)

MR data analysis

The $T1$ and $T2$ relaxation data were analysed, using the Levenberg Marquardt non-linear least squares algorithm. The algorithm was implemented in MatLab (Mathworks, Natick, MA, USA). For each tumor, pixel-by-pixel $T1$ maps were generated from a three-parameter fit of the image intensities according to the equation $S = A + B\ exp(-nTI/T^*1)$. The value of the corrected $T1$ was calculated from the formula: $T1 = T^*1(\mathrm{B/A} - 1))$. Pixel-by-pixel $T2$ maps were generated from fitting the relaxation decays to the monoexponential function: $S = So\ exp(-TE/T2)$, where So the signal amplitude at TE = 0.

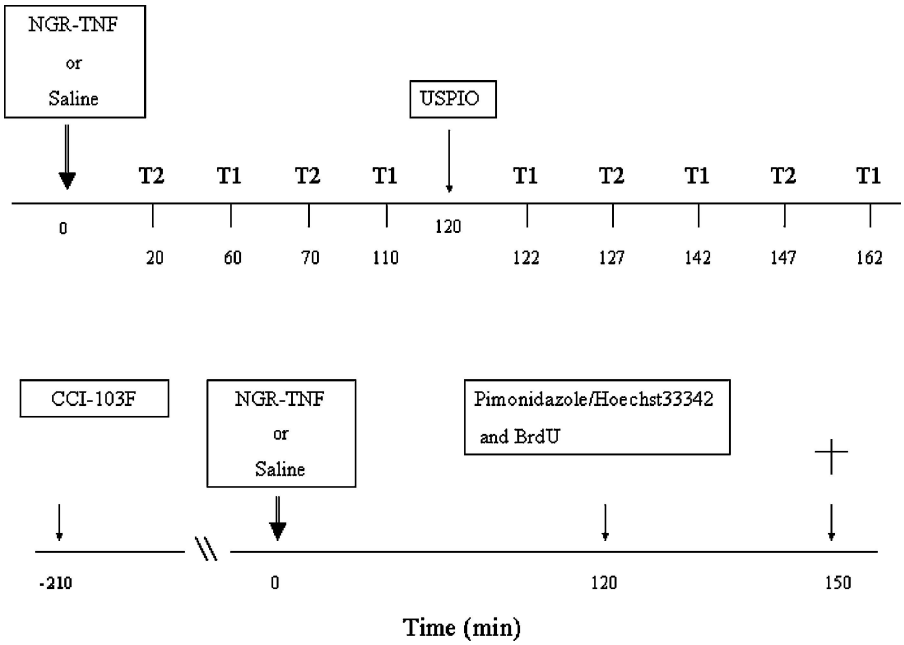

Figure 1. Treatment schedule and experimental design. *Top*. Following NGR-TNF administration in the treated group, or saline in the control group, $T1$ and $T2$ relaxation times were measured as indicated, before and after contrast agent (USPIO) administration. *Bottom*. Immunohistochemical experiments. Animals are killed at time = 150 min. See materials and methods for details.

The details of the $T1$ data analysis are as follows (a similar data analysis was performed for the $T2$ data). For each tumor, five $T1$ maps were obtained, at the two time points (#1 and #2) before USPIO and the three time points (#3, #4 and #5) after USPIO. Two analyses were then performed on the $T1$ maps of the control and treated tumors. In the first analysis, from each map, the mean $T1$ was calculated by drawing an ROI — which includes the whole tumor — on the $T1$ map and averaging the values of all pixels. The values of the mean $T1$ at all time points were then normalized to the value of the first time point. It should be noted that, after USPIO administration, the decrease in $T1$ at time point #3 (just after USPIO) is proportional to the tumor blood volume, while the decrease in $T1$ at time point #4 and #5 (22 and 42 min after USPIO, respectively) is related to USPIO leakage (from the vasculature into the interstitial compartment) and is indicative of vessel permeability/damage. The mean $T1$ relaxation time in the controls was then compared with the mean $T1$ in the treated tumors at each time point. The statistical significance ($p < 0.05$) of the differences between the $T1$ in the control and treated tumor was determined by means of a two-tailed student t-test, using the software package Prism (GraphPad Software Inc., CA, USA).

In the second analysis, histograms of the $T1$ values of all pixels were analyzed as described previously [9]. Briefly, for each tumor a threshold value (TV) was calculated from the formula TV = $\langle T1 \rangle - 1.5$ SD, where $\langle T1 \rangle$ and SD are the mean $T1$ and the standard deviation values, respectively, at time point #1. Then, at all time points, the percentage of pixels that were below this threshold was determined. The statistical significance ($p < 0.05$) of differences between the percentage of pixels below TV in the control and treated tumors was determined by means of a two-tailed student t-test.

Finally, for simplicity, throughout this report the changes in relaxation times ($T1, T2$) will be referred to as being proportional to the blood volume and leakage. Strictly speaking only the changes in relaxation rates (R1= $1/T1$, R2 = $1/T2$) are proportional to the contrast agent concentration. However, since ΔR1,2 are small, a linear relationship exists between ΔR1,2 and $\Delta T1,2$ and thus for the sake of clarity throughout the paper reference will be made to $\Delta T1,2$ instead of ΔR1,2 as index of relative blood volume and leakage.

Markers of hypoxia, perfusion and proliferation

Using immunohistochemical methods the effect of NGR-TNF monotherapy on tumor hypoxia, perfusion and proliferation was studied in a separate group of mice and compared with mice which received normal saline. CCI-103F (1-(2-hydroxy-3-hexafluoroisopropxy-propyl)-2-nitroimidazole, J.A Raleigh, University of North Carolina, Chapel Hill, NC) [17, 18] and pimonidazole (1-((2-hydroxy-3-piperidinyl)propyl)-2-nitroimidazole hydrochloride, Natural Pharmacia International, Belmont, USA) [19–21] were used as hypoxic markers. With the consecutive employment of the two bioreductive markers changes in tumor hypoxia within one tumor can be studied [22]. CCI-103F was dissolved in 10% dimethyl sulfoxide (DMSO) and 90% peanut oil to a concentration

of 4 mg/ml. 0.5 ml of this mixture was injected ip in each mouse 210 minutes before mice were treated with NGR-TNF or normal saline (as described above). Pimonidazole hydrochloride (40 mg/ml) was combined 1:1 with the perfusion marker Hoechst33342 (Serva, Heidelberg, Germany) (7.5 mg/ml). Two hours after treatment 0.1 ml of this solution was injected iv in the tail vein of each mouse. The S-phase marker bromodeoxyuridine (BrdUrd) (Sigma-Aldrich, Zwijndrecht, the Netherlands) (2,5 mg/ml) was injected ip at a dose of 0.5 ml at the same time as the pimonidazole/Hoechst mixture. Again, the 2 hour period was chosen because of the observed maximum effect of NGR-TNF combined with doxorubicin when doxorubicin was administered 2 hours after NGR-TNF. Animals were sacrified by cervical dislocation 30 minutes after injection of pimonidazole/Hoechst and BrdUrd (Figure 1, bottom). Tumors were removed immediately and stored in liquid nitrogen. For staining and further analysis frozen tumor sections of 5 μm thickness were cut.

Immunohistochemical staining

After thawing, the sections were fixed in cold (4°C) acetone for ten minutes. Before immunohistochemical staining of the other markers slides were scanned (see below) for the Hoechst33342 signal. After scanning of the Hoechst33342 signal and between all consecutive steps of the staining procedure sections were rinsed three times for 5 minutes in phosphate buffered saline (PBS). Sections were mounted in Fluorostab (Organon, Boxtel, the Netherlands). The first tissue section was stained for endothelium plus the hypoxic markers CCI and pimonidazole. The next tissue section was stained for endothelium, the second hypoxic marker pimonidazole and the S-phase marker BrdUrd.

Endothelial structures and hypoxic markers

Sections were incubated overnight at 4°C with rabbit anti-CCI-103 (F6) antiserum (J.A. Raleigh) [18, 23] diluted 1:800 in polyclonal liquid dilutant (PLD, Euro-DPC, Breda, the Netherlands). Then sections were incubated during 30 min at 37°C with goat-anti-rabbit-Cy3 (Jackson Immuno Research Laboratories, West Grove, PA, USA), diluted 1:300 in PLD, followed by incubation during 30 min at 37°C with donkey-anti-rabbit-Fab (Jackson) and donkey-anti-mouseFab (Jackson), diluted 1:50 in PLD. Next, sections were incubated with rabbit-anti-pimonidazole (J.A. Raleigh) [20, 24] during 45 min at 37°C diluted 1:800 in PLD, followed by incubation with donkey-anti-rabbit-Alexa488 (Molecular Probes, Leiden, The Netherlands) during 45 min at 37°C diluted 1:400 in PLD. Finally, sections were incubated during 60 min at room temperature with 9F1 (rat monoclonal to mouse endothelium, Department of Pathology, University Medical Centre Nijmegen, the Netherlands 25 followed by incubation during 30 min at 37°C with chicken-anti-rat-Alexa647 (Molecular Probes).

Endothelial structures, pimonidazole and S-phase marker BrdUrd

DNA was denaturized by incubation in 0.2 M HCl during 10 minutes, after which pH was neutralized by rinsing the sections in 0.1 M Borax during 10 min. Then, sections were incubated overnight at 4°C with sheep-anti-BrdUrd (Abcam Ltd, Cambridge, UK) diluted 1:50 in PLD and rabbit-anti-pimonidazole diluted 1:800 in PLD. Next, sections were incubated during 30 min at 37°C with donkey-anti-sheep-Cy3 (Jackson) diluted 1:600 in PLD and donkey-anti-rabbit-Alexa488 diluted 1:400 in PLD. Then, sections were incubated during 60 min at room temperature with 9F1 followed by incubation during 30 min at 37°C with chicken-anti-rat-Alexa647. Finally, all nuclei were stained by incubation of the sections in Fast Blue (Sigma-Aldrich, Zwijndrecht, the Netherlands) diluted 1:1000 in PBS during 15 min at room temperature.

Image analysis

To acquire quantitative data for tumor hypoxia, perfusion and proliferation a semiautomatic method was used, based on a computerised digital image analysis system, as described previously [26, 27]. Each tumor cross-section was scanned with a high-resolution intensified solid-state camera on a fluorescence microscope (Axioskop, Zeiss, Weesp, the Netherlands) using different filters. A computer-controlled motorised stepping stage was used. Each scan consisted of certain number of microscopic fields of 1.2 mm2, depending on the size of the tumor section. After each scan one composite image was reconstructed from the individual microscopic fields. Finally, to delineate the tumor area and exclude non-tumor tissue from the analysis, a contour line was drawn using the corresponding H&E stained slice. The hypoxic fraction (HF) of the tumor section was defined as the surface area stained by the hypoxic marker relative to the viable tumor surface area. The perfused fraction (PF) of the tumor was calculated as the area which was stained both by Hoechst and 9F1 (perfused vascular area) relative to the total vascular area. The relative vascular area (RVA) was obtained by dividing the 9F1 positive area by the viable tumour area and vascular density (VD) was computed as total number of vascular structures per mm2 of viable tumor area. The labelling index (LI) was defined as the ratio of the BrdUrd positive surface and the total nuclear surface.

Statistics and calculations

To compare differences in growth after treatment on each day the *t* test for independent samples was used. To compare

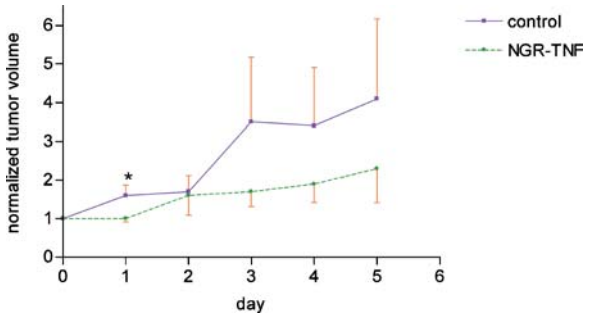

Figure 2. Mean growth of all tumors after NGR-TNF (solid line) compared with mean growth of all tumors after normal saline (dashed line). For each group tumor volumes are normalized to the tumor volume on day 0. Error bars indicate standard error. * $p < 0.05$.

differences in hypoxic fraction, perfused fraction, vascular density and labelling index between different tumors the *t* test for independent samples was used.

Results

Dose-response curves

The growth curves of the tumors after treatment are shown in Figure 2. A significantly smaller mean tumor volume on the first day after treatment with NGR-TNF (5 ng/kg) as a single agent was observed compared with tumor volume after injection of normal saline. No significant differences in tumor volume between the two groups were found before start of the treatment.

MR measurements

The use of a small RF surface coil, in combination with the high magnetic field strength of the MR scanner, yielded high spatial resolution MR images with good signal to noise ratio, despite the small size of the tumors which were investigated in the current study (Figure 3). This enables the quantitative investigation of the relaxation properties of tumors and to assess the changes in relaxation times following contrast agent administration.

All tumors showed a small but consistent increase in the $T1$ relaxation time at the time point #2 (Figure 4). The increase in the $T1$ was statistically significant in the treated group ($p = 0.016$) but not in the control ($p = 0.340$). Just after USPIO administration (time point #3), treated and control animals had similar decrease in $T1$ relaxation time, to the normalized values of 0.971 ± 0.011 and 0.974 ± 0.012, respectively ($p = 0.870$). At the time points #4 and #5, that is, 22 and 42 min after USPIO administration, the $T1$ further decreased in time in the treated group. The $T1$ values after USPIO administration were fitted to a straight line in both control and treated groups. The values of the slope in the treated group was significantly different ($p = 0.028$) than that of the horizontal line (that is, the line which is representative of no contrast agent leakage from the vascular space into the interstitial space); there was no statistically significant difference ($p = 0.367$) between the values of the slope in the control group and than that of the horizontal line.

The percentage of pixels below the $T1$ threshold value (as defined in the materials and methods section) increased with time in both treated and control groups (Figure 5). These values were significantly different between the treated and control tumors at time point #4 (27.6 ± 6.4 and 11.0 ± 1.6, respectively, $p = 0.02$, $N = 5$) and time point #5 (35.4 ± 7.3 and 12.9 ± 2.2, respectively, $p = 0.01$, $N = 5$).

The changes in $T2$ relaxation time in the control and NGR-TNF treated tumors are illustrated in Figure 6. At the time points #4, the $T2$ further decreased in time in the treated group. However, comparison of the $T2$ decrease in treated tumors with that of controls did not show a statistical difference. Histogram analysis of the $T2$ decrease did not show a statistical difference between treated and control tumors.

Immunohistochemical analysis

The hypoxic fraction before treatment was measured by CCI-103F, while after treatment changes in hypoxia were measured by a second marker, pimonidazole, allowing each tumour to serve as its own control. In Figure 7 the relation between vasculature and hypoxic areas before and after treatment is shown. On microscopical observation a considerable overlap between hypoxic areas before and after treatment is noted. In quantitative analysis the control group showed a larger area stained by pimonidazole relative to CCI-103F, as has been published for other tumor models [22]. Therefore, the results were analysed after correction for this difference in staining. Comparing the percentage change in hypoxic fraction before and after injection of NGR-TNF and saline a decrease in hypoxia in NGR-TNF treated animals was observed ($p = 0.059$) (Figure 8).

In Figure 9 the relation between vasculature, hypoxic areas and proliferation is shown. On microscopical observation a considerable amount of proliferative activity is observed in hypoxic areas. The quantitative analysis showed that in the control group on average 22.1% of the viable tumor area consisted of proliferating cells and 5.1% of these proliferating cells were hypoxic. Comparing the control group with the NGR-TNF treated group an increase in labeling index was observed after NGR-TNF treatment ($p = 0.082$), as well as an increase in the percentage of proliferating cells that were hypoxic ($p = 0.022$) (Figure 10).

No differences were found between the control group and the NGR-TNF treated group with respect to the viable tumor area, the fraction of perfused vessels, the relative vascular area and vascular density.

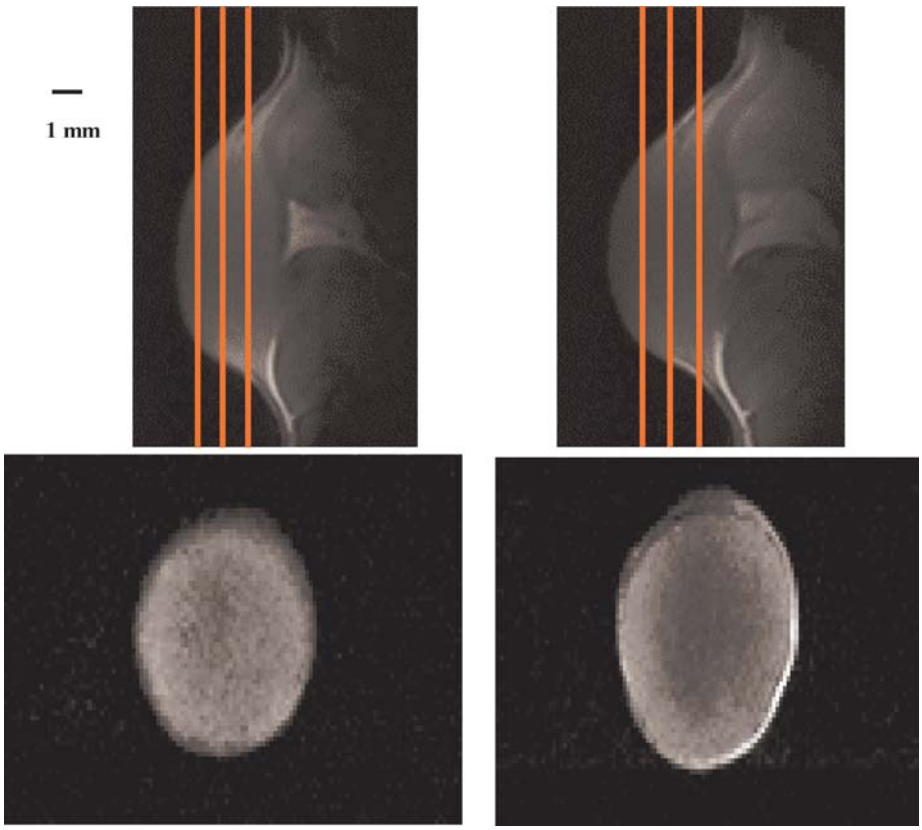

Figure 3. MR images of RMA lymphoma. *Top*. Two sagittal spin echo $T2$-weighted images, with in plane resolution of 120 × 120 μm. The red lines on the sagittal images indicate the position and thickness (1 mm) of the axial images. *Bottom*. Axial $T2$-weighted images, with in plane resolution of 240 × 240 μm.

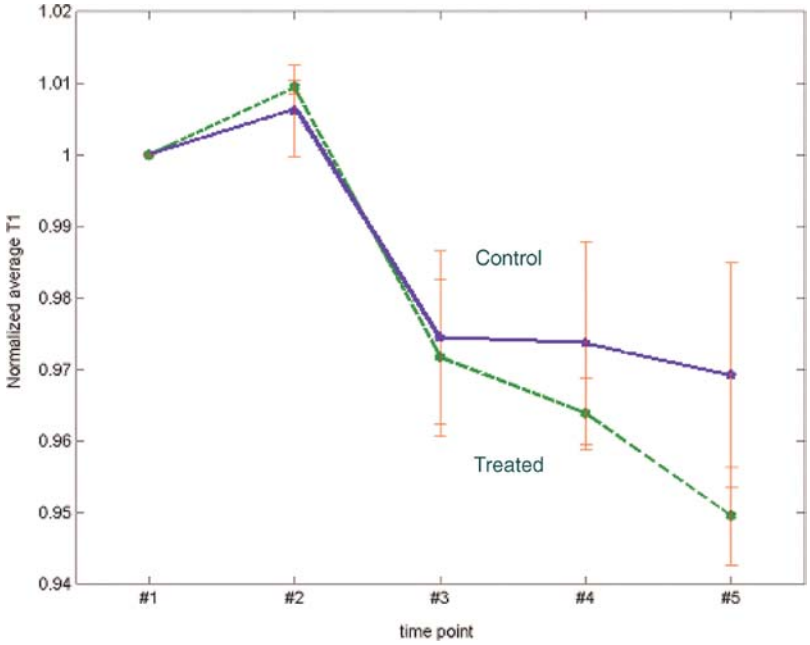

Figure 4. Plot of the normalized average T_1 at the two time points (#1 and #2) before USPIO and the three time points (#3, #4 and #5) after USPIO administration, in treated and control groups. After USPIO, the decrease in T_1 is more pronounced in the treated than in control group. However, there were no statistically significant differences between the treated animals and controls at any time point. Error bars indicate standard errors.

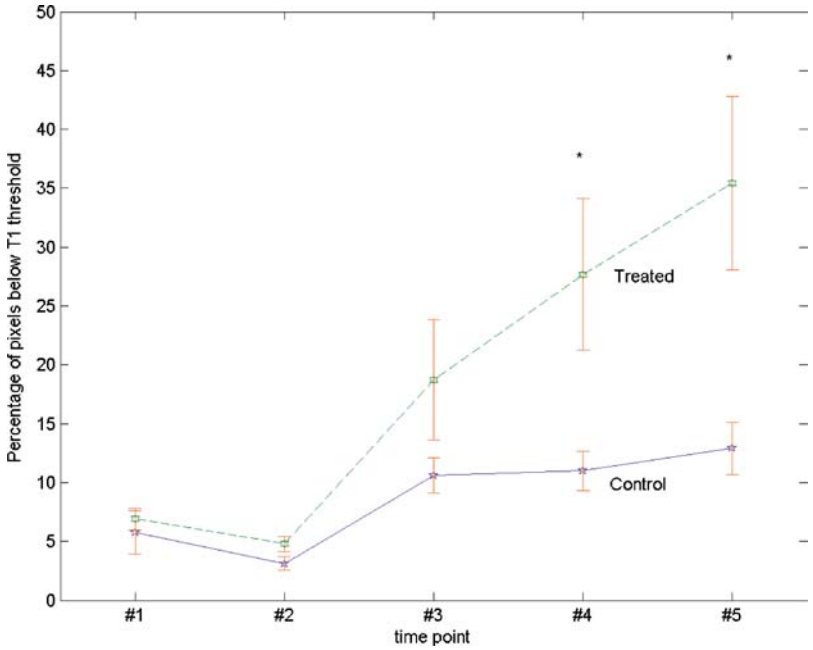

Figure 5. The percentage of pixels below the T_1 threshold value (as defined in the materials and methods section), before (time points #1 and #2) and after (time points #3, #4 and #5) USPIO administration. The percentage value increased with time after USPIO administration in both control and treated groups. These values were significantly different between the treated and control tumors at time point #4 (27.6 ± 6.4 and 11.0 ± 1.6, respectively, $p = 0.02$, $N = 5$) and time point #5 (35.4 ± 7.3 and 12.9 ± 2.2, respectively, $p = 0.01$, $N = 5$).

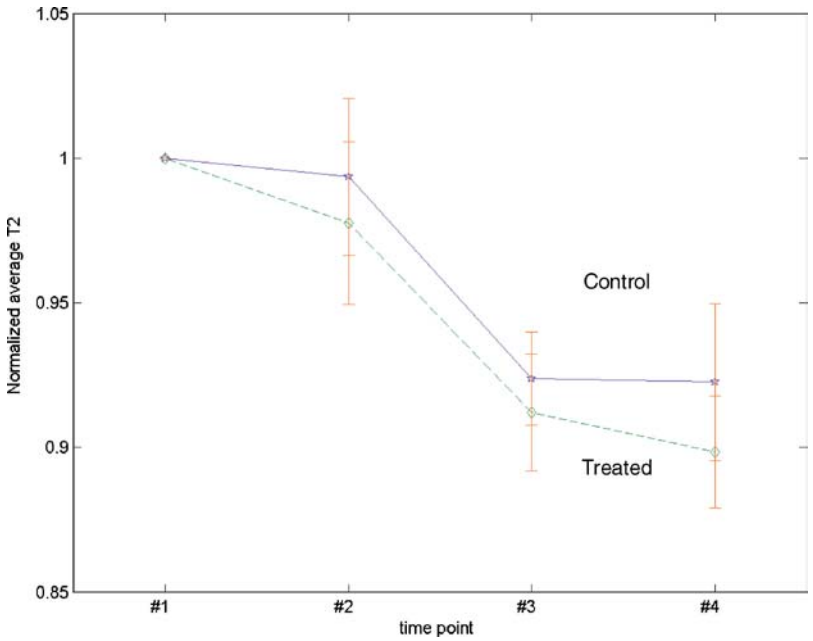

Figure 6. Plot of the normalized average T_2 at two time points (#1 and #2) before USPIO and two time points (#3, #4) after USPIO administration, in treated (dashed line) and control (solid line) groups. There were no statistically significant differences between the treated animals and controls at any time point.

Discussion

An effect of NGR-TNF (5 ng/kg) on tumor growth was observed one day after treatment administration, despite the relatively large standard error of the mean (s.e.m.) on our growth curves. This relatively large s.e.m. is a reflection of differences in growth pattern (infiltrative or superficial) which can be observed in this lymphoma line. The effect of low doses of NGR-TNF on tumor growth one day after treatment has also been reported previously [7].

No differences in $T1$ and $T2$ relaxation times were found between treated and control tumors directly after USPIO

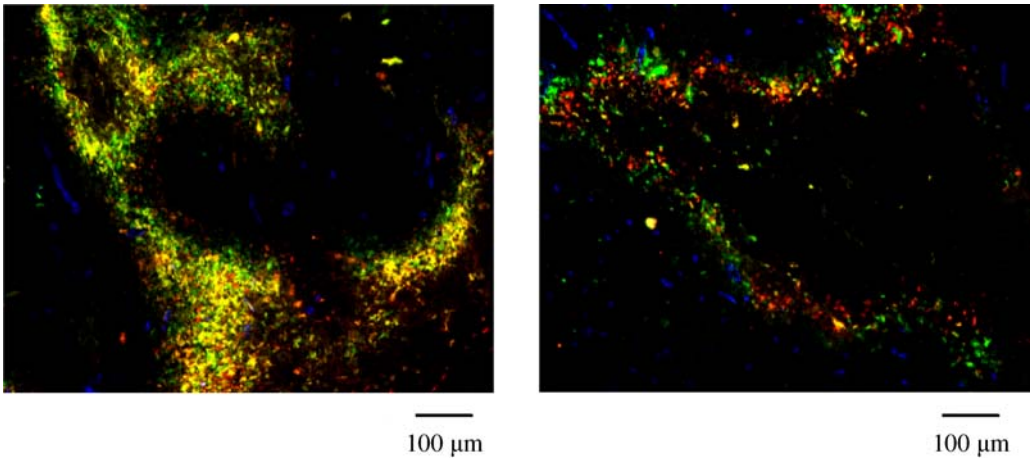

Figure 7. Photomicrograph of a detail of RMA-T lymphoma of the control group (*left*) and the group treated with NGR-TNF (*right*) showing vasculature and hypoxic areas. Vascular structures: blue; hypoxic areas stained by CCI-103 F: red; hypoxic areas stained by pimonidazole: green; overlap of CCI-103F and pimonidazole stained areas: yellow.

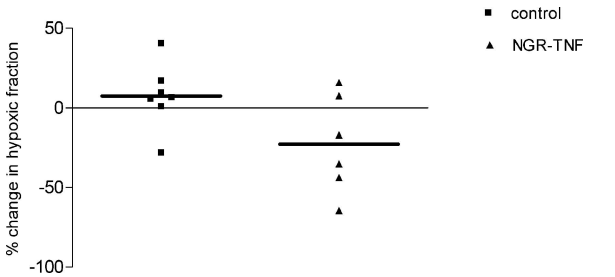

Figure 8. Plot showing the percentage change in hypoxia fraction, calculated by the difference in pimonidazole stained area minus CCI-103F stained area divided by the CCI-103F stained area, for the control and the NGR-TNF treated group.

administration. Since the decrease in relaxation times just after USPIO is proportional to the tumor blood volume, NGR-TNF does not seem to influence blood volume within this time frame. The decrease of $T1$ (and $T2$) further in time (#4 and #5, Figure 4, 6) is due to an increase in the amount of contrast agent within the imaged pixels, which can be attributed to extravasation of the contrast agent from the vascular space into the interstitial space. Although it cannot be excluded that an increase in blood volume also played a role, a doubling of blood volume after NGR-TNF -which is highly unlikely- would have been necessary to explain our results. Since the number of pixels with increased USPIO content is higher in the treated than in the control group, this strongly suggests leakage of the USPIO from the vasculature to the interstitial space, indicating a NGR-TNF-induced vessel damage and/or increased vessel permeability. Although the changes in $T2$ relaxation times were consistent with the observed changes in $T1$ relaxation time, they did not show a statistical difference. This could be attributed to the lower sensitivity of $T2$ relaxation time to USPIO. Moreover, $T2$ relaxation time measurements are more sensitive to motion artifacts than the $T1$ relaxation time measurements and, as a result, are characterized by a lower precision.

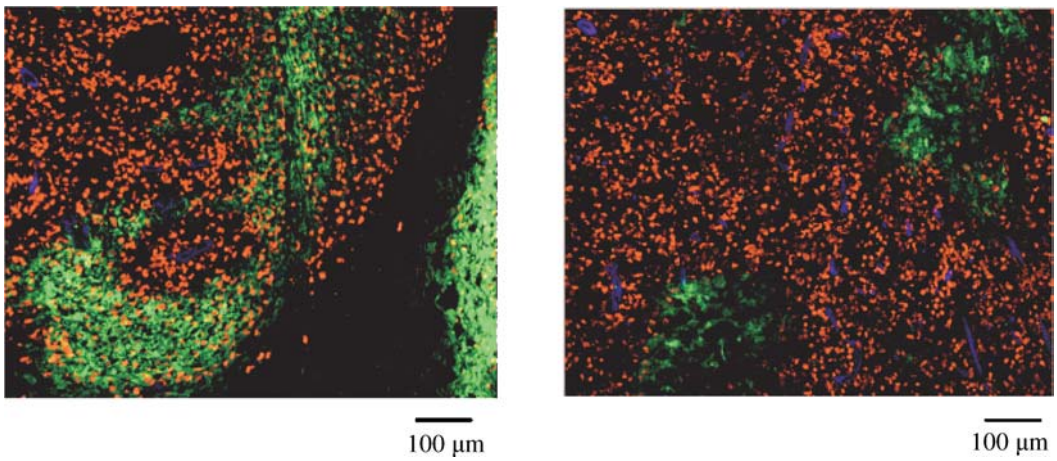

Figure 9. Photomicrograph of a detail of RMA-T lymphoma of the control group (*left*) and the group treated with NGR-TNF (*right*) showing vasculature, hypoxic areas and proliferation. Vascular structures: blue; hypoxic areas stained by pimonidazole: green; proliferation: red.

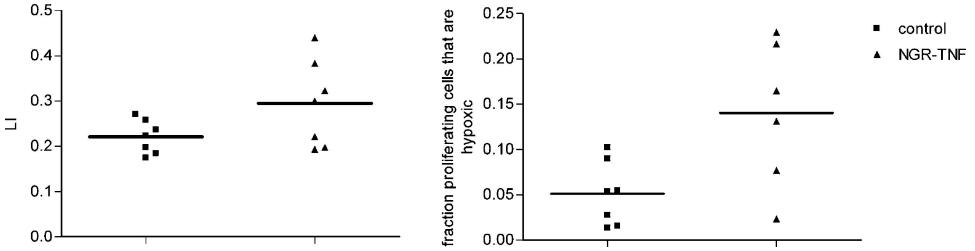

Figure 10. Plot showing the BrdUrd labeling index (*left*) and the fraction of proliferating cells that are hypoxic (*right*) for the control and the NGR-TNF treated group.

After NGR-TNF treatment a decrease in tumor hypoxia and an increase in BrdUrd labeling index was observed, both for the whole tumor area and for hypoxia areas. The decrease in hypoxic fraction in the tumor may be explained by either an increased delivery of oxygen to the tumor or a decrease in oxygen consumption by the tumor. The first explantion seems more likely, since the increase in BrdUrd LI denotes increased proliferation which is compatible with an increase in oxygen consumption. An increased delivery of oxygen could be caused by increased tumor blood flow, as has been described previously for low dose (1–10 μg/kg) TNF treatment of carcinosarcoma tumors [28]. Therefore, an increase in oxygen delivery to the tumor may explain the observed increase in proliferation. In fact, low dose TNF (1–10 μg/kg) treatment of carcinosarcoma tumors [28] stimulated tumor growth, although the authors explained the increase in tumor size by a pronounced immigration of host cells, predominantly polymorphonuclear leukocytes. Increased proliferation might also be a direct effect of TNF on tumor cells, since in vitro experiments have shown enhanced proliferation rates in normal cells after treatment with TNF [29].

From a therapeutic perspective a decrease in tumor hypoxia and an increase in labeling index may be detrimental, possibly leading to increased tumor growth. However, in combination with other therapeutic agencies the decrease in tumor hypoxia may be beneficial. Several studies have shown for the superior effect of radiotherapy in combination with hypoxia decreasing agents compared with radiotherapy as single treatment [30]. Moreover, our growth experiments have shown a decrease in tumor growth one day after NGR-TNF treatment. Apparently, the effects on tumor hypoxia and proliferation two hours after treatment are transient and overruled by other, possibly more longlasting, effects. For example, the increase in vascular permeability that was observed in our MR experiments may lead to haemoconcentration and an increase in interstitial pressure, ultimately resulting in an reduction of tumor blood flow [28] and thus in a decrease in tumor growth. Therefore, a beneficial effect of NGR-TNF in combination with other therapeutical agents may critically depend on the sequence and timing of the regimens. Currently, a phase I study with NGR-TNF as a single agent is ongoing in patients with solid tumors and combination studies with chemotherapy are being planned.

Acknowledgments

The authors thank B. Lemmers, I. Elemans, G. Grutters and colleagues at the Central Animal Laboratory for biotechnical assistance and animal care.

This study was financially supported by MolMed S.p.A., Milano, Italy.

References

1. van der Veen AH, de Wilt JH, Eggermont AM, van Tiel ST, Seynhaeve AL, ten Hagen TL: TNF-alpha augments intratumoural concentrations of doxorubicin in TNF-alpha-based isolated limb perfusion in rat sarcoma models and enhances anti-tumour effects. Br J Cancer 82:973–980, 2000
2. Kristensen CA, Nozue M, Boucher Y, Jain RK: Reduction of interstitial fluid pressure after TNF-alpha treatment of three human melanoma xenografts. Br J Cancer 74:533–536, 1996
3. Suzuki S, Ohta S, Takashio K, Nitanai H, Hashimoto Y: Augmentation for intratumoral accumulation and anti-tumor activity of liposome-encapsulated adriamycin by tumor necrosis factor-alpha in mice. Int J Cancer 46:1095–1100, 1990
4. Eggermont AM, Schraffordt KH, Lienard D, Kroon BB, van Geel AN, Hoekstra HJ, Lejeune FJ: Isolated limb perfusion with high-dose tumor necrosis factor-alpha in combination with interferon-gamma and melphalan for nonresectable extremity soft tissue sarcomas: A multicenter trial. J Clin Oncol 14:2653–2665, 1996
5. Lejeune FJ: High dose recombinant tumour necrosis factor (rTNF alpha) administered by isolation perfusion for advanced tumours of the limbs: A model for biochemotherapy of cancer. Eur J Cancer 31A:1009–1016, 1995
6. Curnis F, Sacchi A, Borgna L, Magni F, Gasparri A, Corti A: Enhancement of tumor necrosis factor alpha antitumor immunotherapeutic properties by targeted delivery to aminopeptidase N (CD13). Nat Biotechnol 18:1185–1190, 2000
7. Curnis F, Sacchi A, Corti A: Improving chemotherapeutic drug penetration in tumors by vascular targeting and barrier alteration. J Clin Invest 110:475–482, 2002
8. Kauppinen RA: Monitoring cytotoxic tumour treatment response by diffusion magnetic resonance imaging and proton spectroscopy. NMR Biomed 15:6–17, 2002
9. Duvvuri U, Poptani H, Feldman M, Nadal-Desbarats L, Gee MS, Lee WM, Reddy R, Leigh JS, Glickson JD: Quantitative T1rho magnetic resonance imaging of RIF-1 tumors in vivo: Detection of early response to cyclophosphamide therapy. Cancer Res 61:7747–7753, 2001
10. Dennie J, Mandeville JB, Boxerman JL, Packard SD, Rosen BR, Weisskoff RM: NMR imaging of changes in vascular morphology due to tumor angiogenesis. Magn Reson Med 40:793–799, 1998

11. Le Duc G, Peoc'h M, Remy C, Charpy O, Muller RN, Le Bas JF, Decorps M: Use of T(2)-weighted susceptibility contrast MRI for mapping the blood volume in the glioma-bearing rat brain. Magn Reson Med 42:754–761, 1999
12. Tropres I, Grimault S, Vaeth A, Grillon E, Julien C, Payen JF, Lamalle L, Decorps M: Vessel size imaging. Magn Reson Med 45:397–408, 2001
13. Robinson SP, Rijken PF, Howe FA, McSheehy PM, van der Sanden BP, Heerschap A, Stubbs M, van der Kogel AJ, Griffiths JR: Tumor vascular architecture and function evaluated by non-invasive susceptibility MRI methods and immunohistochemistry. J Magn Reson Imaging 17:445–454, 2003
14. Bremer C, Mustafa M, Bogdanov A, Jr., Ntziachristos V, Petrovsky A, Weissleder R: Steady-state blood volume measurements in experimental tumors with different angiogenic burdens a study in mice. Radiology 226:214–220, 2003
15. Pathak AP, Rand SD, Schmainda KM: The effect of brain tumor angiogenesis on the in vivo relationship between the gradient-echo relaxation rate change (DeltaR2*) and contrast agent (MION) dose. J Magn Reson Imaging 18:397–403, 2003
16. Moro M, Pelagi M, Fulci G, Paganelli G, Dellabona P, Casorati G, Siccardi AG, Corti A: Tumor cell targeting with antibody-avidin complexes and biotinylated tumor necrosis factor alpha. Cancer Res 57:1922–1928, 1997
17. Raleigh JA, Franko AJ, Treiber EO, Lunt JA, Allen PS: Covalent binding of a fluorinated 2-nitroimidazole to EMT-6 tumors in Balb/C mice: Detection by F-19 nuclear magnetic resonance at 2.35 T. Int J Radiat Oncol Biol Phys 12:1243–1245, 1986
18. Raleigh JA, Miller GG, Franko AJ, Koch CJ, Fuciarelli AF, Kelly DA: Fluorescence immunohistochemical detection of hypoxic cells in spheroids and tumours. Br J Cancer 56:395–400, 1987
19. Durand RE, Raleigh JA: Identification of nonproliferating but viable hypoxic tumor cells in vivo. Cancer Res 58:3547–3550, 1998
20. Arteel GE, Thurman RG, Yates JM, Raleigh JA: Evidence that hypoxia markers detect oxygen gradients in liver: Pimonidazole and retrograde perfusion of rat liver. Br J Cancer 72:889–895, 1995
21. Raleigh JA, Chou SC, Arteel GE, Horsman MR: Comparisons among pimonidazole binding, oxygen electrode measurements, and radiation response in C3H mouse tumors. Radiat Res 151:580–589, 1999
22. Ljungkvist AS, Bussink J, Rijken PF, Raleigh JA, Denekamp J, van der Kogel AJ: Changes in tumor hypoxia measured with a double hypoxic marker technique. Int J Radiat Oncol Biol Phys 48:1529–1538, 2000
23. Cline JM, Thrall DE, Page RL, Franko AJ, Raleigh JA: Immunohistochemical detection of a hypoxia marker in spontaneous canine tumours. Br J Cancer 62:925–931, 1990
24. Azuma C, Raleigh JA, Thrall DE: Longevity of pimonidazole adducts in spontaneous canine tumors as an estimate of hypoxic cell lifetime. Radiat Res 148:35–42, 1997
25. Westphal JR, van't Hullenaar RG, van der Laak JA, Cornelissen IM, Schalkwijk LJ, van Muijen GN, Wesseling P, de Wilde PC, Ruiter DJ, de Waal RM: Vascular density in melanoma xenografts correlates with vascular permeability factor expression but not with metastatic potential. Br J Cancer 76:561–570, 1997
26. Bussink J, Kaanders JH, Rijken PF, Martindale CA, van der Kogel AJ: Multiparameter analysis of vasculature, perfusion and proliferation in human tumour xenografts. Br J Cancer 77:57–64, 1998
27. Rijken PF, Bernsen HJ, van der Kogel AJ: Application of an image analysis system to the quantitation of tumor perfusion and vascularity in human glioma xenografts. Microvasc Res 50:141–153, 1995
28. Kallinowski F, Schaefer C, Tyler G, Vaupel P: In vivo targets of recombinant human tumour necrosis factor-alpha: Blood flow, oxygen consumption and growth of isotransplanted rat tumours. Br J Cancer 60:555–560, 1989
29. Sugarman BJ, Aggarwal BB, Hass PE, Figari IS, Palladino MA, Jr., Shepard HM: Recombinant human tumor necrosis factor-alpha: Effects on proliferation of normal and transformed cells in vitro. Science 230:943–945, 1985
30. Kaanders JH, Bussink J, van der Kogel AJ: ARCON: A novel biology-based approach in radiotherapy. Lancet Oncol 3:728–737, 2002

Address for offprints: H.W.M. van Laarhoven (MD, MA), Department of Medical Oncology, University Medical Centre Nijmegen, PO Box 9101, 6500 HB, Nijmegen, The Netherlands. Tel.: +31 24 361 52 15, Fax: +31 24 354 07 88; E-mail: h.vanlaarhoven@onco.umcn.nl